Helmholtz-Zentrum Geesthacht
Zentrum für Material- und Küstenforschung

Final Draft
of the original manuscript:

Dorado-Linan, I.; Sanchez-Lorenzo, A.; Gutierrez Merino, E.; Planells, O.; Heinrich, I.; Helle, G.; Zorita, E.:

Changes in surface solar radiation in Northeastern Spain over the past six centuries recorded by tree-ring Delta13C

In: Climate Dynamics (2015) Springer

DOI: 10.1007/s00382-015-2881-x

Changes in surface solar radiation in Northeastern Spain over the past six centuries recorded by tree-ring $\delta^{13}C$

I. Dorado-Liñán[1]*, A. Sanchez-Lorenzo[2], E. Gutiérrez Merino[3], O. Planells[3], I. Heinrich[4], G. Helle[4], E. Zorita[5]

[1]Technische Universität München. Ecoclimatology. München, Germany
[2]Instituto Pirenaico de Ecología, Consejo Superior de Investigaciones Científicas (IPE–CSIC). Zaragoza, Spain
[3]Universitat de Barcelona. Departamentd'Ecologia. Barcelona,Spain
[4]GFZ, German Research Centre for Geosciences. Climate Dynamics and Landscape Evolution.Potsdam,Germany
[5]Helmholtz-Zentrum-Geesthacht. Institute for Coastal Research.Geesthacht, Germany

Correspondence to:I. Dorado-Liñán(dorado@wzw.tum.de)

Abstract

Although solar radiation at the surface plays a determinant role in carbon discrimination in tree rings, stable carbon isotope chronologies ($\delta^{13}C$) have often been interpreted as a temperature proxy due to the co-variability of temperature and surface solar radiation. Furthermore, even when surface solar radiation is assumed to be the main driver of ^{13}C discrimination in tree rings, $\delta^{13}C$ records have been calibrated against sunshine duration or cloud cover series for which longer observational records exists. In this study, we use different instrumental and satellite data over northeast Spain (southern Europe) to identify the main driver of tree-ring ^{13}C discrimination in this region. Special attention is paid to periods in which the co-variability of those climate variables may have been weaker, such as years after large volcanic eruptions. The analysis identified surface solar radiation as the main driver of tree-ring $\delta^{13}C$ changes in this region, although the influence of other climatic factors may not be negligible. Accordingly, we suggest that a reconstruction of SSR over the last 600 years is possible. The relation between multidecadal variations of an independent temperature reconstruction and surface solar radiation in this region shows no clear sign, and warmer (colder) periods may be accompanied by both higher and lower surface solar radiation. However, our reconstructed records of surface solar radiation reveals a sunnier Little Ice Age

in agreement with other $\delta^{13}C$ tree-ring series used to reconstruct sunshine duration in central and northern Europe.

1. Introduction

Surface solar radiation (SSR or global radiation) may change as a response to a perturbation of the climate system, for instance, due to anthropogenic greenhouse gases, as the amount of cloud cover or the radiative properties of clouds may respond to changes in atmospheric temperatures (Stevens and Bony 2013). Climate models still show significant discrepancies in the simulation of the response of clouds to climate change (Stephens et al. 2005; Boucher et al. 2013). The uncertainties in the simulation of cloudiness and SSR are still the single most important reasons for the large spread in the climate sensitivity among climate models (Dessler 2010; Flato et al. 2013).

It is known that SSR has not been constant through time and since the mid-20th century it has experimented a widespread declining phase (dimming period) followed by an increasing phase (brightening period)(Stanhill and Cohen 2001; Wild et al. 2005; Wild 2012). Among the possible causes of these changes in SSR are anthropogenic and natural aerosols, aerosol-cloud interactions and variation in cloudiness induced by the internal variability of the climate system (Wild 2009 and references therein). These changes in SSR should have an effect on surface temperatures (Wild et al. 2007; Wang and Dickinson 2013). On the other hand, changes in surface temperatures may affect SSR through induced changes in cloudiness (Dessler 2010). Part of the difficulties in disentangling the mutual interaction between variations in SSR and temperature are due to the short length of the existing instrumental SSR series (Wang and Dickinson 2013).

The use of related variables for which longer observational series exists (Román et al. 2014; Wild et al. 2007; Makowski et al. 2009;Wang and Dickinson 2013) have allowed the extension of the SSR inferences back a few decades, but not before the 20th century in most of the cases. The relations between the changes in temperature and the associated changes in SSR at the timescales involved in climate change could be better assessed if the period of analysis could be extended back in time covering climatic periods where temperatures may have considerably differed from the present climate, such as the Little Ice Age (LIA) or be roughly similar to 20th century temperatures as in the Medieval Climate Anomaly (MCA).

The availability of natural proxy records, such as those traditionally used to reconstruct temperature and precipitation (i.e., tree rings, lake sediments, ice cores), allows the assessment of longer-term changes than would be unfeasible just using observational data. In this context, the autotrophic metabolism of plants that depends on temperature, moisture and the incident sunlight (Farquhar et al. 1982, 1989) points to tree rings as one of the very few terrestrial archives that could potentially be used to assess past changes in sunlight-related variables. Although the stable carbon isotopes in tree rings ($\delta^{13}C$) are the outcome of an interplay of several factors, the capacity to encode changes in sunlight has been recently demonstrated for Scandinavia (Young et al. 2010, 2012; Gagen et al. 2011; Loader et al. 2013) and in the Alps (Hafner et al. 2014).

Such an approach was possible because plant growth relies on the production of carbohydrates from water and CO_2 in a light-dependent process, in which the rate of photosynthetic fixation depends on light intensity. The discrimination of ^{13}C in organic matter (i.e, tree rings) reflects the balance between the leaf photosynthetic rate and the stomatal conductance of CO_2 (Farquhar et al. 1982, 1989), which are strongly dependent on environmental variables such as temperature, humidity, and solar radiation. Briefly stated, in water-limited environments discrimination of ^{13}C is theoretically driven by moisture-induced limitations of stomatal conductance, while under non-limiting moisture conditions ^{13}C discrimination would mainly be controlled by photosynthetic rate driven by solar radiation (Farquhar et al. 1989; McCarrol and Loader 2004).

Although these physiological processes are theoretically understood, the scarcity and limited length of available instrumental SSR records favour the misinterpretation of tree-ring $\delta^{13}C$ as temperature proxy (Gagen et al. 2007). This scarcity may also have restricted the option to calibrate $\delta^{13}C$ chronologies to sunlight variables with longer observational records than SRR, such as sunshine duration hours (SD) or percentage of cloud cover (CC)(Young et al. 2012; Gagen et al. 2011; Loader et al. 2013;Hafner et al. 2014). As a consequence, $\delta^{13}C$ have been used to reconstruct climate variables which *a priori* may not be the primary drivers of isotopic fractionation.

The reconstruction of indirect drivers of $\delta^{13}C$ would not be incorrect as long as the relationship between the main and the indirect driver has not changed in time. Specifically, temperature reconstructions based on $\delta^{13}C$ assume a linear relationship between SSR and temperature over the whole reconstruction period. However, the major modulator of SSR at interannual scales is cloudiness. Cloudiness can contribute either to cooling i.e. low-level clouds promoting higher albedo; or to warming, i.e. high clouds emit less infrared radiation out to the space (e.g., Mace et al. 2006), which can compromise a linear relationship to surface temperature. In addition, the relationship between temperature and cloudiness may depend on which of these two is the driving factor and which is passively responding. At interannual timescales, cloudiness is likely modulating the local temperature, particularly in summertime at mid-latitudes, but at multidecadal timescales, CC and cloud type may respond to large-scale multidecadal temperature changes (Dessler 2010).

Similarly, the $\delta^{13}C$-based SD/CC reconstructions, although physically more closely related to SSR than temperature, have additional shortcomings. Both, SSR and the part of the SSR used by plants for photosynthesis (the so-called photosynthetic active radiation, PAR) comprise both direct and diffuse fractions. Diffuse fraction may play a determinant role in sustaining photosynthetic activity when the direct fraction is low (Mercado et al. 2009), which occurs under decreased atmospheric transmittance such as cloudy skies or with increased concentration of atmospheric aerosols (e.g., large volcanic eruptions). SD and CC records do not take into account the diffuse fraction of the SSR. Thus, under non-clear skies SD/CC may differ from SSR (e.g., Sanchez-Romero et al. 2014).

In order to identify the main driver of $\delta^{13}C$ variations in tree rings, special attention needs to be paid to periods in which these climate variables may have diverged. In this context, the perturbation caused by volcanic eruptions may lead to diverging responses between temperature sensitive and sunlight sensitive tree-ring records (Battipalgia et al. 2007). Large volcanic events may cause a large-scale cooling which is detectable locally in instrumental series and in temperature sensitive tree-ring records, such a tree-ring width or maximum density (D'Arrigo et al. 2013). However, the volcanically induced local cooling may not strongly affect the photosynthetic capacity of the tree, which translates in no or non-significant changes in tree-ring $\delta^{13}C$ (Battipaglia et al. 2007).

In this study we use a 600-years long $\delta^{13}C$ tree-ring chronologyfrom a non-moisture-limited site at the eastern Pre-Pyrenees (Spain, Southwestern Europe)where net primary production is potentially constrained by SSR (Nemani et al. 2003) and take advantage of a dense network of station and satellite-derived SSR, SD, CC, and air temperature records located in the vicinity of the sampling site. Our goal is to empirically identify the main driver of ^{13}C discrimination in tree rings and for that purpose we also specially focus on periods where large volcanic eruptions occurred. Once SSR is identified as the main driver of $\delta^{13}C$, we use the long tree-ring $\delta^{13}C$ chronology to reconstruct SSR over the last centuries at this site. Finally we discuss the relation to the historical changes in temperature and the agreements with other $\delta^{13}C$ records encoding sunlight related signals in Europe.

2. Material and methods

2.1. Site description and chronology development

The study site is an east-facing slope sub-alpine forest of *Pinusuncinata* Ram. located at 2120 m.a.s.l. in the Cadí-Pedraforca Range (UPF), eastern Pre-Pyrenees (Fig. 1a). Mean annual temperature is 6.1ºC and total annual rainfall is over 1000 mm, with more than 300 mm of precipitation falling evenly in June, July and August (Fig. 1b) due to the advection of humid air masses coming from the Mediterranean Sea (Planells et al. 2006). Low temperatures mark the beginning and end of the growing season and moisture is not a limiting factor for treeradial growth(Fig. 1c). Thus, the determinant control on carbon isotope fractionation is likely to be photosynthetic rate rather than stomatal conductance (McCarrol and Loader 2004).

During summer of 2006, a total amount of 75 cores were taken from living trees using increment borers. The samples were mounted, dried and sanded until individual cells were visible under the stereomicroscope. Cores were visually cross-dated following standard dendrochronological techniques (Stokes and Smiley 1968). Tree-ring widths were measured and quality and correct dating of the resulting series checked with the COFECHA software (Holmes 1983).

For the stable carbon isotope measurements, nine trees were selected and the individual rings separated with a razor-blade under a microscope. Due to the critical size of the tree rings produced by the older trees in the most recent centuries, using the same trees to cover the full period was unfeasible. Thus, four trees were selected to cover the period 1600-1900 and the oldest five trees were chosen to cover the period 1600-backwards (Fig. 2a). The period 1550-1600 was individually measured in every sample to ensure a correct overlap.Similarly, the 20^{th} century was also individually analyzed. The rest of the chronology was build using a combination of pooled and individual measurements every fifth year in order to meet time and costs constraints usually associated with stable isotope measurements, while allowing annual resolution and an estimation of signal replication.

Diverse studies have shown that pooling the cores can yield similar results to those obtained analyzing individual samples (Treydte et al. 2001; Leavitt and Long, 1984; McCarrol and Loader 2004). The similarity of the results obtained by these two methodological approaches was successfully tested in Dorado Liñán et al. (2011) for the data used in this chronology. Cellulose was extracted from entire rings (early- and latewood) using standard techniques (Boettger et al. 2007). Carbon isotope analysis was conducted on carbon dioxide resulting from combustion of the samples in an elemental-analyzer and an isotope-ratio mass-spectrometer (McCarroll and Loader 2004). Isotope values are given as $\delta^{13}C$ -values calculated from the isotope ratios $^{13}C/^{12}C$ (= R) as $\delta^{13}C$ = (Rsample/Rstandard – 1)*1000‰ (referring to the international standard VPDB), and have a long-term estimated methodological error of <0.2‰ (Boettger et al. 2007).

We applied the atmospheric correction to the $\delta^{13}C$ series to correct for the decreasing trend of atmospheric CO_2 signature due to the increasing fossil fuel burning depleted in ^{13}C since the industrialization (see details and values in McCarroll and Loader 2004). The corrected $\delta^{13}C$ individual series were transformed to z-scores before averaging them into a site chronology

The resulting $\delta^{13}C$ chronology from the Cadí-Pedraforca Range (UPF $\delta^{13}C$) displays a robust common signal over the period 1332-2006 CE (Fig. 2a). UPF $\delta^{13}C$ chronology displays a typical positive co-variability to summer temperature and a negative correlation with summer precipitation (Figure 2b). Such a signal is common even in sites known not to suffer from moisture limitations (e.g., Gagen et al. 2007; Saurer et al 2008). According to moist characteristic of UPF and the lack of a drought signal on tree growth, the negative correlation with precipitation may reflect the relation to other factor inversely related to precipitation such as SD or SSR.

2.2. Instrumental data

Different sources of monthly mean SD, CC, SSR, and mean air temperature (T) were considered in this study (Fig. 1a). The records of SSR were extracted from Sanchez-Lorenzo et al. (2013a, 2013b), whereas SD and CC databases were obtained from Sanchez-Lorenzo et al. (2007) and Sanchez-Lorenzo et al. (2012), respectively. The reader is referred to those studies for further technical details, including instrumentation, temporal homogenization, and gap filling. In addition, SSR derived from the Satellite Application Facility on Climate Monitoring (CM SAF) has been extracted over Europe with a spatial resolution of 0.03° × 0.03° for the period 1983–2005 (Posselt et al. 2012). For an unbiased evaluation of the climatic influences, the common period for all series 1983-2005 was used for further analysis. Additionally, centennial-long temperature (BaT) and percentage of cloud cover (BaCC) instrumental series were available from the Barcelona station (41.39N; 2.7E).

For further comparisons and assessment of the link between temperature and $\delta^{13}C$, this study takes advantage of the established May-to-September temperature reconstruction at the Pyrenees (PyrT) based in maximum latewood density (MXD) (Dorado Liñán et al. 2012), as well as the Scandinavian summer CC reconstruction (ScanCC; Young et al., 2012) and April-to-August temperature reconstruction (ScanT; Melvin et al. 2012) based on $\delta^{13}C$ and MXD, respectively. It is worth mentioning that MXD usually encodes the temperature signal of the full growing season, while $\delta^{13}C$ tends to encode summer climate signals. Therefore, the temperature and sunlight reconstruction that will be compared do not strictly described the same season.

2.3. Data analysis

Previous studies used SD records to calibrate sunlight sensitive tree-ring $\delta^{13}C$ chronologies because the short length of the common period when using SSR records hinders a split-sample procedure. In our particular case, the longest SSR record available starts in 1968 CE (Millau station) and the shortest begins in 1983 CE (La Molina, Barcelona, Girona, Huesca and Lleida). The inclusion of SSR records in the analysis starting in 1983 CE limits the common period for all series to 1983-2005. An additional calibration-verification test with the few records reaching back 1976 CE has been included in the supplementary material.In every case, the calibration-verification tests have been performed by the leave-one-out cross-validation. The linear relationship between the instrumental records and the UPF $\delta^{13}C$ was evaluated by the adjusted R^2 (R^2_{adj}) and predicted R^2 (R^2_{pred}) derived from every cross-validation. The autocorrelation of regression residuals required to estimate the significance of the regression coefficients was estimated by the Durbin-Watson test.

The effect of large volcanic eruption in long instrumental series as well as in temperature and sunlight-sensitive tree-ring variables was tested by Superposed Epoch Analysis (SEA) (Panofsky and Brier 1958). The evaluation of the volcanic imprint was done in two steps. First, the assessment of the large volcanic eruptions in temperature and sunlight-related variables was tested on the long instrumental records from Barcelona BaT and BaCC. For the SEA analysis on these series, eight large volcanic eruptions from 1866 CE to 1995 CE in both Northern and Southern Hemispheres were considered: 1883, 1888, 1902, 1912, 1963, 1980, 1982 and 1991. Secondly, we run SEA analyses on UPF $\delta^{13}C$ and the available reconstructions PyrT, ScanCC and ScanT. SEA analyses were performed with three different sets of volcanic eruptions in order to account for the uncertainty in the dating of volcanic events. We used the subsets from (1) D'Arrigo et al. (2013); (2) Stine and Huybers (2014), which is derived from Gao et al. (2008) and; (3) a collection of seven volcanic eruptions that took place during the last two centuries from Gao et al. (2008). The analysis was performed using DplR (Bunn 2008) and the statistical significance of the signal was tested using bootstrapping (e.g., Fischer et al. 2007; D'Arrigo et al. 2009).

3. Results

3.1. Driver of $\delta^{13}C$ variations at UPF

The correlations between stable carbon isotopes and monthly T, SD, CC and SSR identify the summer months June, July and August (JJA) as the dominating climate season for tree growth (Fig. 3, left panel). Higher (lower) summer T, SD and SSR (CC) are linked to a significant ($p<0.05$) positive (negative) response of tree-ring $\delta^{13}C$. The comparison of the different set of JJA instrumental records and the individual $\delta^{13}C$ series (Fig. 3, right panel) evidences that the different T series have a more similar interannual variability than the records within each set of SD, CC and SSR series. Furthermore, the comparison also discloses disagreements in their trends. While the T records show a common and significant upward trend ($p< 0.05$) during this period, the records of SD, CC, SSR and $\delta^{13}C$ series do not exhibit such a marked trend. Particularly, $\delta^{13}C$ and the CC records do not show any significant trend, while two out of 10 SSR records (Mallorca and Huesca) and three out of the eight SD records (Mallorca, Madrid, Lleida) display significant trends.

Two major volcanic eruptions took place during the last three decades: El Chichón (1982) and Pinatubo (1991). However, two events are not enough to draw statistically robust conclusions about the impact of these perturbations on instrumental records and $\delta^{13}C$. The availability of longer T and CC records from the Barcelona station allows for a longer-term analysis of the effect of large volcanic eruptions on the tree-ring and instrumental variables (Fig. 4, top). During the period from 1866 CE to 1995 CE, eight large volcanic eruptions with radiative impact on both hemispheres occurred. The SEA revealed a significant negative impact ($p<0.01$) of volcanic eruptions on T while no significant impact was observed on CC or on $\delta^{13}C$ in this region (Fig. 4, bottom).

The linear regression models between UPF $\delta^{13}C$ and each of the different collections of observational climate data show higher explained variance (R^2adj) when using SSR series as predictors than T, SD or CC (Table 1 and Fig. 5). Furthermore, the linear regression performed with SSR series as predictor display similar amounts of explained and predicted variance (R^2pred), while the low predictive skills of regression using T and SD denotes model overfitting. Although most of the regressions do not show significant autocorrelation of the residuals (Fig. 6), the significant trend detected in the residuals of most of the regression models performed with T further supports the hypothesis that a relevant predictor may be missing in these models.

Among the collections of observational records in the vicinity of the sampling site (Fig. 7), the SSR series from La Molina (50km distance) provide the best fit to $\delta^{13}C$ (R^2adj=64.1%) and the highest predictive skills (R^2pred=58.5%) among all models. Furthermore, the regression residuals for SSR show no significant trend (p=0.15). The T record from the nearby station La Molina also displays a good fit (R^2adj=61.7%) but the lower predictive skills (R^2pred=49.9%) denotes once more model overfitting. Regarding the CC and SD, the best fit corresponds to the station of Madrid (600km distance). In the case of SD, the R^2adj and R^2pred are slightly higher than those described for the SSR station La Molina. However, the long distance between the station and the sampling site and the fact that none of the closer stations gives similar results points to spurious correlations. When extending the common calibration-verification period back to 1976, the number of records available in the vicinity of the sampling site is dramatically reduced. However, models using SSR records still display better fits than temperature records (see Fig. 1 and Table 1 from supplementary material). Therefore, we conclude that the SSR data are best reflecting the real forcing factor of $\delta^{13}C$ variability at this site, and consequently interpret the variations of $\delta^{13}C$ tree-ring chronology spanning the period 1332-2006CE as the results of the changes in sunlight (PyrSSR, hereafter).

3.2. Changes in sunlight for the last 600 years

The comparison of this PyrSSR record and the preexisting growing season temperature reconstruction at the Pyrenees PyrT (Fig.8) further illustrates the inconsistency of interpreting

$\delta^{13}C$ as a temperature record at this site, although both recordsdo not strictly represent the same season (see Section 2.2). The historical variations of PyrT and PyrSSR reveal no clear sign of linear relationship between growing season temperature and summer SSR at this site. For example, both records markedly anticorrelate during periods such as the one spanning from around 1600 to 1800 CE. Increased summer SSR was related to both periods of cooler and warmer growing season temperatures. Specifically, the period from the 14th to the 16th century was characterized by generally warmer temperatures but alternating periods of higher or lower SSR. During the second half of the Spörer minimum (first half of the 16th) temperatures were less warm than during previous century and the SSR was also lower. From the end of the 16th century until the end of the 18th century temperatures were gradually decreasing while SSR was high, except for a reduction during the Maunder minimum which coincides with a period of decreased total solar irradiance (TSI). The lowest temperatures during LIA occurred during the Dalton Minimum and coincide with a minimum in summer SSR associated to a marked decrease in TSI. Despite the reduced SSR duringthe Dalton Minimum, the LIA is generally related to higher SSR. From this period until the second half of the 20th century, the climate at the Pyrenees was characterized by low SSR and a gradual increase in temperatures. The 20th century shows a maximum in temperatures during the first half of the century and low SSR, increasing during the last decades in line with the global warming and brightening periods described in the literature (e.g., Wild et al. 2007).

The comparison with the historical summer CC and growing season temperature reconstructions from Scandinavia (ScanCC and ScanT, respectively), also shows a common pattern of cloudiness during the central part of the LIA (Fig.8). ScanCC displays a persistent decrease in summer CC from the beginning of the 17th century until the end of the 18th century which is consistent with the sunnier summer period described for the Pyrenees. Although different patterns of summer cloudiness/SSR are observed before the 17th century and after the 19th century, both sites show a common response of summer cloudiness/SSR and growing season temperature to large volcanic eruptions. The three SEA performed with different sets of volcanic eruptions do not show evidence of a significant impact of large volcanic eruptions on ScanCC and PyrSSR, while volcanic eruptions generally exert a significant cooling impact ($p<0.05$) on the MXD based temperature reconstructions ScanT and PyrT in the same year and over a few years after the eruption.

4. Discussion

The correlations of UPF $\delta^{13}C$ and monthly T, CC, SD and SSR indicate a close link of summer climatic conditions and tree growth, but also reveal high co-variance among all four meteorological variables. The short length of the SSR records, which limits the common period of analysis, and the fact that only two major volcanic eruptions occurred during this period, hinders the unequivocal attribution of changes in $\delta^{13}C$ to one main climatic driver. However, linear regression models performed for the different sets of climate variables reveal the better explaining and predictive skills of the SSR models and the larger spatial significance of the relationship between UPF $\delta^{13}C$ and SSR. In addition, the test on the volcanic imprint on the long instrumental records from Barcelona BaT and BaCC and the UPF $\delta^{13}C$ identified a significant effect (cooling) attributable to volcanic eruptions in BaT, whereas no clear volcanic signal could be detected in BaCC and UPF $\delta^{13}C$, strongly suggesting that temperature changes are not the main driver of $\delta^{13}C$ variations in tree rings at UPF.

Proxy records encoding temperature signals are expected to display a significant change in the values after large volcanic eruptions as a consequence of the decrease in local temperatures that usually follows these events (D'Arrigo et al., 2013). In contrast, as shown by the pioneer study by Battipaglia et al. (2007), large volcanic eruptions producing a regional to global significant cooling did not lead to a significant reduction of tree photosynthetic rates in Italy. Accordingly, the interpretation of UPF $\delta^{13}C$ as non-temperature proxy record is further supported by the lack of a significant volcanic imprint over the last six centuries, regardless of the sub-sample of volcanic eruptions considered, while PyrT displays significant decreases in temperatures in the year of the eruption and in a few subsequent years. Thus, major volcanic events during the last six centuries reduced tree growth at the Pyrenees probably by inducing a decrease in temperatures that may have shortened the growing season. However, neither the reduction of the length of the growing season nor the increased concentration of stratospheric aerosols did affect the $\delta^{13}C$ record, which we interpret as a lack of influence of volcanic eruptions on summer photosynthetic activity at this site.

This lack of impact of volcanic eruptions on $\delta^{13}C$ may seem puzzling at first sight, but in theory the $\delta^{13}C$ record reflects the PAR and not totally reflects SSR. According to the hypothesis of the diffuse SSR/PAR-compensation proposed by Mercado et al. (2009), the reduction in direct PAR due to increases in clouds or aerosols is compensated by the increase of the diffuse fraction of PAR, which may explain the lack of a significant volcanic imprint in $\delta^{13}C$. Although the diffuse SSR (PAR) may not always totally compensate the reduction on the direct SSR (PAR) (e.g., Ogle et al., 2005), this approach provides a useful test-bed to disentangle the role of the diffuse radiation in maintaining the photosynthetic rate under low-transmittance skies. Nonetheless, the hypothesis of the diffuse light compensation may not be the only reason for the maintenance of the photosynthetic rates. Changes in cloudiness or atmospheric aerosol (such as those induced by volcanic eruptions) may not only alter the direct/diffuse fractions, but also the ratio PAR/SSR reaching the surface. The limited availability of direct measurements of PAR causes that PAR records are often estimated as a fix proportion of SSR. However, such a proportion is known to change under lower transmittance conditions since clouds, dust and aerosols shows higher transparency to PAR (0.4-0.7μm) than to other fractions of the SSR spectrum such as the infrared wavebands (0.7 to 1.7 μm) (Papaioannou et al., 1993; Jacovides et al., 2003; Bat-Oyun et al., 2012). Thus, the lack of significant changes on $\delta^{13}C$ under cloudy and dusty conditions derived from volcanic eruptions may be due to either the increase in the diffuse fraction of PAR, or to the general increase of the PAR/SSR ratio.

From a long-term perspective, the comparison of the 600-year long PyrSSR and reconstructed temperatures at the Pyrenees (PyrT) evidences periods of anomalies of opposite sign, such as during the LIA. The fact that PyrT describes the variations of a longer season than PyrSSR would not explain the observed differences, which again highlights the physical inconsistency of interpreting $\delta^{13}C$ as a temperature proxy at this site. The relationship between past growing season temperature and past summer SSR at this site is complex, with no clear linear relationship, similar to the results reported in Scandinavia by Gagen et al. (2011).

The increase in summer SSR observed in ScanCC and PyrSSR during the recent decades is in line with the widespread surface brightening observed since the 1980s (Wild, 2009; Wild, 2012), which also has been observed in Spain (Sanchez-Lorenzo et al., 2007, 2013b). However, this brightening period was exceeded by far during the LIA, when both records ScanCC and PyrSSR show sunnier summers than nowadays. These results also agree with those described in Scandinavia (Gagen et al., 2011, Loader et al., 2013) and in the Alps (Hafner et al., 2014). Thus, colder growing season temperatures in Scandinavia, Alps and Pyrenees during LIA were associated to higher summer SSR. While lower temperatures during the LIA have been associated to the lower TSI and the increased concentration in atmospheric aerosols as a result of periods of volcanism (Crowley, 2000; Miller et al., 2012), the mechanism driving SSR changes are not clear yet. Loader et al. (2013) did the first attempt and related the cold and sunny period during LIA in Fennoscandia to persistent anti-cyclonic conditions due to the dominance of Arctic and maritime air masses. At this point, we can only speculate about the dynamical processes that gave rise to the increase of SRR during the LIA in these three regions. The fact that all of them display a similar signal during a cold periodmaybe indicating an overall reduction of evaporation from the ocean as a result of lower sea-surface-temperatures. The accompanying reduction in summer cloud cover over continental Europe could be the main factor rather than changes in large-scale atmospheric circulation.

5 Conclusions

The joint analysis of instrumental records of different variables related to incoming sunlight, near-surface temperature and $\delta^{13}C$ tree-ring chronology located in Northeast Spain (Southern Europe), indicates that SSR plays a major role among the drivers of summer carbon fractionation in tree-rings in this region. Also, the SEA applied to different sets of volcanic eruptions and the comparison between the long $\delta^{13}C$ chronology and temperature reconstructions from this region, rules out $\delta^{13}C$ as a temperature proxy. We thus interpret the centennial $\delta^{13}C$ record as an indicator of past SSR which allowed the reconstruction of incoming sunlight over the last 600 years.

The relationship between past temperature and past SSR at the Pyrenees shows no clear relationship through the 600 years as for example temperature and SSR were positively correlated during the MCA but anticorrelated during the LIA.

Overall, the comparison across the existing tree-ring $\delta^{13}C$ records encoding sunlight-related signals revealed that the brightening phase since 1980s is not unprecedented in the context of the last centuries and LIA appears as a sunnier period in the different tree-ring $\delta^{13}C$ records.

Our results show the potential of using volcanic eruptions to discern the $\delta^{13}C$ chronologies that could potentially be used to extend the geographical coverage of reconstructions of incoming sunlight, contributing to better a understanding of the interaction between past temperatures and SSR on continental scales, a key parameter contributing to global climate sensitivity.

Acknowledgments

The research was funded by the EU-project MILLENNIUM (017008-2), EU-project ISONET (Contract EV K2 = 2001-00237). ASL was supported by a postdoctoral fellowship JCI-2012-12508 and the projects CGL2014-55976-R and CGL2014-52135-C3-01-R from the Spanish Ministry of Economy and Competitiveness. EZ contribution is part of the Cluster of Excellence CLISAP funded by the German Science Foundation. The authors would like to thank the two anonymous reviewers for their constructive comments. Data from this paper is available and can be accessed through the corresponding author.

References

Bat-Oyun T, Shinoda M, Tsubo M (2012) Effects of cloud, atmospheric water vapor, and dust on photosynthetically active radiation and total solar radiation in a Mongolian grassland. J Arid Land 4(4): 349-356.

Battipaglia G, Cherubini P, Saurer M, Siegwolf RTW, Strumia S, Cotrufo, MF (2007) Volcanic explosive eruptions of the Vesuvio decrease tree ring growth but not photosynthesis rates in the surrounding forest. Glob Change Biol 13: 1122-1137.

Boucher O, Randall D, Artaxo P, Bretherton C, Feingold G, Forster P, Kerminen VM, Kondo Y, Liao H, Lohmann U, Rasch P, Satheesh SK, Sherwood S, Stevens B, Zhang XY (2013) Clouds and aerosols. In Climate Change 2013: The Physical Science Basis. Contribution of Working Group I to the Fifth Assessment Report of the Intergovernmental Panel on Climate Change, T.F. Stocker, D. Qin, G.-K. Plattner, M. Tignor, S.K. Allen, J. Doschung, A. Nauels, Y. Xia, V. Bex, and P.M. Midgley, Eds. Cambridge University Press, 571-657, doi:10.1017/CBO9781107415324.016.

Bunn A (2008) A dendrochronology program library in R (dplR).Dendrochronologia 26(2): 115–124.

D'Arrigo R, Wilson R, Tudhope A (2009) Impact of volcanic forcing on tropical climate during the past five centuries. Nat Geosci 2: 51–56. doi:10.1038/NGE0393.

D'Arrigo R, Wilson R, Anchukaitis KJ (2013) Volcanic cooling signal in tree ring temperature records for the past millennium. J Geophys Res: Atmospheres 118(16): 9000–9010.

Dessler AE (2010) A determination of the cloud feedback from climate variations over the past decade. Science 330: 1523–1527.

Dorado Liñán I, Gutierrez E, Helle G, Heinrich I, Andreu-Hayles L, Planells O, Leuenberger, M, Bürger C, Schleser G (2011) Pooled versus separate measurements of tree-ring stable isotopes. Sci Total Environ 409: 2244-2251.

Dorado Liñán I, Büntgen U, González-Rouco F, Zorita E, Montávez JP, Gómez-Navarro JJ, Brunet M, Heinrich I, Helle G, Gutiérrez E (2012) Estimating 750 years of temperature variations and uncertainties in the Pyrenees by tree-ring reconstructions and climate simulations. Clim Past 8(3): 919–933.

Farquhar GD, O'Leary MH, Berry JA (1982) On the relationship between carbon isotope discrimination and intercellular carbon dioxide concentration in leaves. Austral J Plant Physiol 9: 121–137.

Farquhar GD, Ehleringer JR, Hubick KT (1989) Carbon Isotope Discrimination and Photosynthesis.Annu Rev Plant Physio Plant Mol. Biol, 40: 503-537. DOI: 10.1146/annurev.pp.40.060189.002443.

Flato G, Marotzke J, Abiodun B, Braconnot P, Chou SC, Collins W, Cox P, Driouech F, Emori S, Eyring V., Forest C, Gleckler P, Guilyardi E, Jakob C, Kattsov V, Reason C, Rummukainen M (2013) Evaluation of Climate Models. In: Climate Change 2013: The Physical Science Basis. Contribution of Working Group I to the Fifth Assessment Report of the Intergovernmental Panel on Climate Change [Stocker, T.F., D. Qin, G.-K. Plattner, M. Tignor, S.K. Allen, J. Boschung, A. Nauels, Y. Xia, V. Bex and P.M. Midgley (eds.)], Cambridge University Press, Cambridge, United Kingdom and New York, NY, USA.

Fischer EM, Luterbacher J, Zorita E, Tett SFB, Casty C, Wanner H (2007) European climate response to tropical volcanic eruptions over the last half millennium. Geophys Res Lett 34: L05707. doi:10.1029/2006GL027992.

Gagen M, McCarroll D, Loader NJ, Robertson I, Jalkanen R, Anchukaitis KJ (2007) Exorcising the 'segment length curse': summer temperature reconstruction since AD 1640 using non-detrended stable carbon isotope ratios from pine trees in northern Finland. The Holocene, 17: 435–446.

Gagen M, Zorita E, McCarroll D, Young GHF, Grudd H, Jalkanen R, Loader NJ, Robertson I, Kirchhefer AJ (2011) Cloud response to summer temperatures in Fennoscandia over the last thousand years. Geophys Res Lett 38: L05701. doi: 10.1029/2010GL046216.

Gao CC, Robock A, Ammann C (2008) Volcanic forcing of climate over the past 1500 years: an improved ice corebased index for climate models. J Geophys Res 113: D23111.

Hafner P, McCarroll D, Robertson I, Loader N, Gagen M, Young G, Bale R, Sonninen E, and Levanič T (2014) A 520 year record of summer sunshine for the eastern European Alps based on stable carbon isotopes in larch tree rings. ClimDyn 43(3-4): 971-980. doi:10.1007/s00382-013-1864-z.

Holmes RL (1983) Computer-assisted quality control in tree-ring dating and measurement. Tree-Ring Bulletin 43: 69-78.

Jacovides CP, Tymvios FS, Asimakopoulos DN, Theofilou KM, Pashiardes S (2003) Global photosynthetically active radiation and its relationship with global solar radiation in the Eastern Mediterranean basin. TheorApplClimatol 74:227–233.

Leavitt SW, Long A (1989) Drought indicated in carbon-13/carbon-12 ratios of southwestern tree rings. Water Resour Bull. 25: 341-347.

Loader NJ, Young GHF, Grudd H, McCarroll D (2013) Stable carbon isotopes from Torneträsk, northern Sweden provide a millennial length reconstruction of summer sunshine and its relationship to Arctic circulation. Quaternary Sci Rev 62: 97–113.

Mace GG, Benson S, Kato S (2006) Cloud radiative forcing at the Atmospheric Radiation Measurement Program Climate Research Facility: 2. Vertical redistribution of radiant energy by clouds. J Geophys Res, 111:D11S91. doi:10.1029/2005JD005922.

Makowski K, Wild M, Ohmura A (2008) Diurnal temperature range over Europe between 1950 and 2005.AtmosChemPhys 8: 7051–7084.

Matuszko D (2012) Influence of cloudiness on sunshine duration.Int J Climatol 32: 1527–1536.

Melvin TM, Grudd H, Briffa KR (2012)Potential bias in 'updating' tree-ring chronologies using regional curve standardisation: Re-processing 1500 years of Torneträsk density and ring-width data.The Holocene (2013) 23: 364-373.Doi: 10.1177/0959683612460791

Mercado LM, Bellouin N, Sitch S, Boucher O, Huntingford C, Wild M, Cox PM (2009) Impact of Changes in Diffuse Radiation on the Global Land Carbon Sink. Nature 458: 1014-1018.

McCarroll D, Loader NJ (2004) Stable isotopes in tree rings. QuaternSci Rev 23: 771–801.

Nemani RR, Keeling CD, Hashimoto H, Jolly WM, Piper SC, Tucker CJ, Myneni RB, RunningSW (2003) Climate-driven increases in global terrestrial net primary production from 1982 to 1999. Science, 300: 1560–1563.

Ogle N, Turney CSM, Kalin RM, O'Donnell L, Butler CJ (2005) Palaeovolcanic forcing of short-term dendroisotopic depletion: The effect of decreased solar intensity on Irish oak. Geophys Res Lett, 32.doi: 10.1029/2004GL021623. issn: 0094-8276.

Panofsky HA, Brier GW (1958) Some Applications of Statistics to Meteorology. Pa. State Univ. Press, University Park.

Papaioannou G, Papanikolaou N, Retalis D (1993) Relationships of photosynthetically active radiation and shortwave irradiance. TheorApplClimatol 48: 23–27.

Planells O, Andreu L, Bosch O, Gutiérrez E, Filot M, Leuenberger M, Helle G, Schleser GH (2006) The potential of stable isotopes to record aridity conditions in a forest with low-sensitive ring widths from eastern Pre-Pyrenees. In: Heinrich I, Gärtner H, Monbaron M, Schleser G (eds.) (2006) TRACE - Tree Rings in Archaeology, Climatology and Ecology, 4: 266–272.

Posselt R, Mueller R, Stöckli R, Trentmann J (2012) Remote sensing of solar surface radiation for climate monitoring - The CM-SAF retrieval in international comparison. Remote Sens Environ 118: 186–198.

Román R, Bilbao J, de Miguel A (2014) Reconstruction of six decades of daily total solar shortwave irradiation in the Iberian Peninsula using sunshine duration records. Atmos Environ 99: 41–50. DOI: 10.1016/j.atmosenv.2014.09.052.

Sanchez-Lorenzo A, Brunetti M, Calbo J, Martin-Vide J (2007) Recent spatial and temporal variability and trends of sunshine duration over the Iberian Peninsula from a homogenized dataset. J Geophys Res 112: D20115. doi:10.1029/2007JD008677.

Sanchez-Lorenzo A, Calbó J, Wild M (2012) Increasing cloud cover in the 20th century: review and new findings in Spain. Clim Past 8: 1199-1212.

Sanchez-Lorenzo A, Wild M, Trentmann J (2013a) Validation and stability assessment of the monthly mean CM SAF surface solar radiation data set over Europe against a homogenized surface dataset (1983-2005). Remote Sens Environ 134: 355–366.

Sanchez-Lorenzo A, Calbó J, Wild M (2013b) Global and diffuse solar radiation in Spain: building a homogeneous dataset and assessing their trends. Glob Planet Chang 100: 343- 352.

Sanchez-Romero A, Sanchez-Lorenzo A, Calbó J, González JA, Azorin-Molina C (2014) The signal of aerosol-induced changes in sunshine duration records: A review of the evidence. J Geophys Res: Atmospheres 119 (8): 4657–4673.

Stanhill G, Cohen S (2001) Global dimming: a review of the evidence for a widespread and significant reduction in global radiation with discussion of its probable causes and possible agricultural consequences. Agr Forest Meteorol 107: 255-278.

Stephens GL (2005) Cloud feedbacks in the climate system: a critical review. Journal of Climate 18: 237-273.

Stevens B, Bony S (2013) What are climate models missing? Science 344:1053–1054. doi:10.1126/science.1237554.

Stine AR, Huybers P (2014) Arctic tree rings as recorders of variations in light availability, Nature Comms 5: 3836. doi: 10.1038/ncomms4836.

Stokes MA, Smiley TL (1968) Introduction to tree-ring dating. Chicago, IL, USA: University of Chicago Press.

Suehrcke H, Bowden RS, Hollands KGT (2013) Relationship between sunshine duration and solar radiation. Solar Energy 92: 160–171.

Treydte K, Schleser GH, Schweingruber FH, Winiger M (2011) The climatic significance of $\delta^{13}C$ in subalpine spruces (Lötschental, SwissAlps). Tellus 53B: 593–611.

Wang KC, Dickinson RE (2013) Contribution of solar radiation to decadal temperature variability over land. PNAS 110(37): 14877–14882. doi: 10.1073/pnas.1311433110.

Wild M, Gilgen H, Roesch A, Ohmura A, Long C, Dutton E, Forga B, Kallis A, Russak V, Tsvetkov A (2005) From dimming to brightening: Decadal changes in solar radiation at the Earth's surface. Science 308: 847-850.

Wild M, Ohmura A, Makowski K (2007) Impact of global dimming and brightening on global warming. Geophys Res Lett 34: L04702. doi:10.1029/2006GL028031.

Wild M (2009) Global dimming and brightening: A review. J Geophys Res 114: D00D16. doi:10.1029/2008JD011470.

Wild M (2012) Enlightening Global Dimming and Brightening. Bull Am MeteorolSoc, 93(1): 27–37. doi:10.1175/BAMS-D-11-00074.1.

Young GHF, McCarroll D, Loader NJ, Kirchhefer AJ (2010) A 500-year record of summer near-ground solar radiation from tree-ring stable carbon isotopes. Holocene 20(3): 315–324.

Young G, McCarroll D, Loader N, Gagen M, Kirchhefer A, Demmler J (2012) Changes in atmospheric circulation and the Arctic Oscillation preserved within a millennial length reconstruction of summer cloud cover from northern Fennoscandia. ClimDyn 39(1-2): 495-507. doi:10.1007/s00382-011-1246-3.

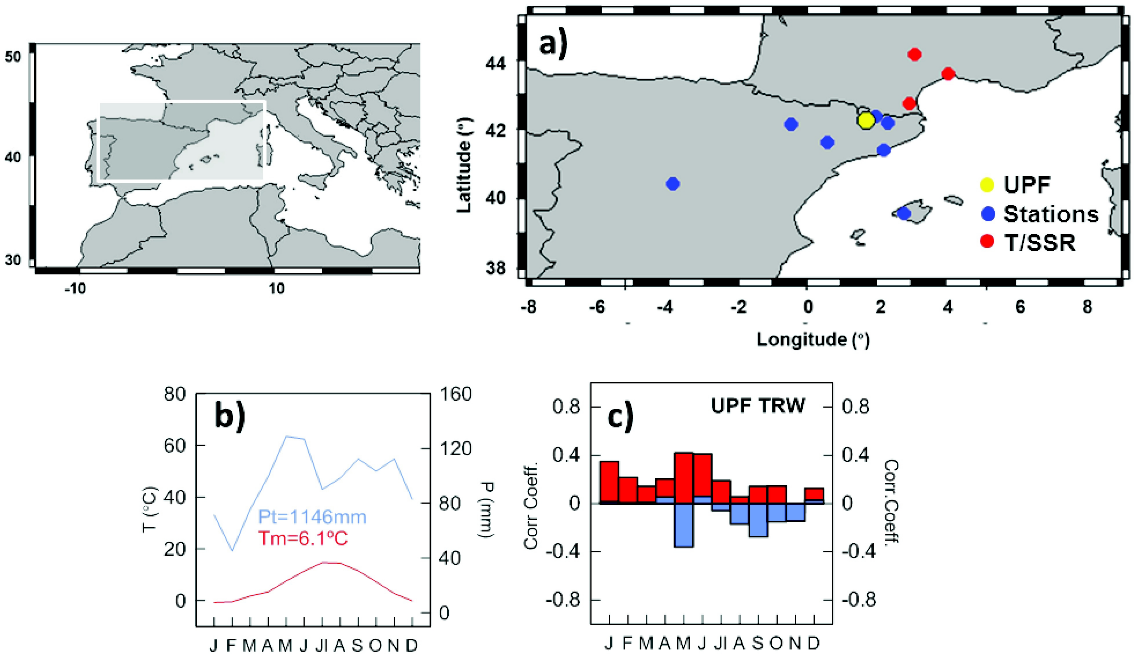

Fig. 1 a) Location of the Pedraforca site (UPF, yellow dot) and the meteorological stations of temperature (T), surface solar radiation (SSR), sunshine duration (SD) and percentage of cloud cover (CC) (blue dots). Red dots correspond to additional stations from which T and SSR were available but not CC and SD. Bottom graph shows the b) climatogram (mean temperature and precipitation) of the closest station to the sampling site (La Molina) and; c) correlations of the UPF tree ring-width chronology (UPF TRW) with mean temperature (red) and precipitation (blue) from La Molina.

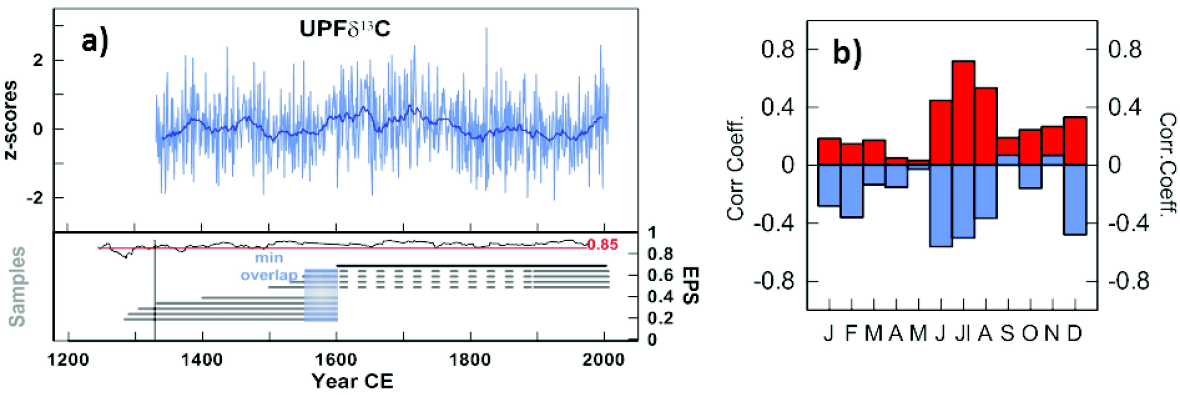

Fig. 2 Stable carbon isotope chronology from UPF (UPF δ^{13}C). a) Final composite chronology spanning the period 1332-2006 CE and the periods covered by each individual tree series. Red line marks the 0.85 expressed-population-signal threshold computed with the individually measured samples using a 150-yrs running window. Blue shaded area highlight the overlap period of the samples extending the chronology further back in time and; b) correlations of UPF δ^{13}C with temperature (red) and precipitation (blue) from La Molina.

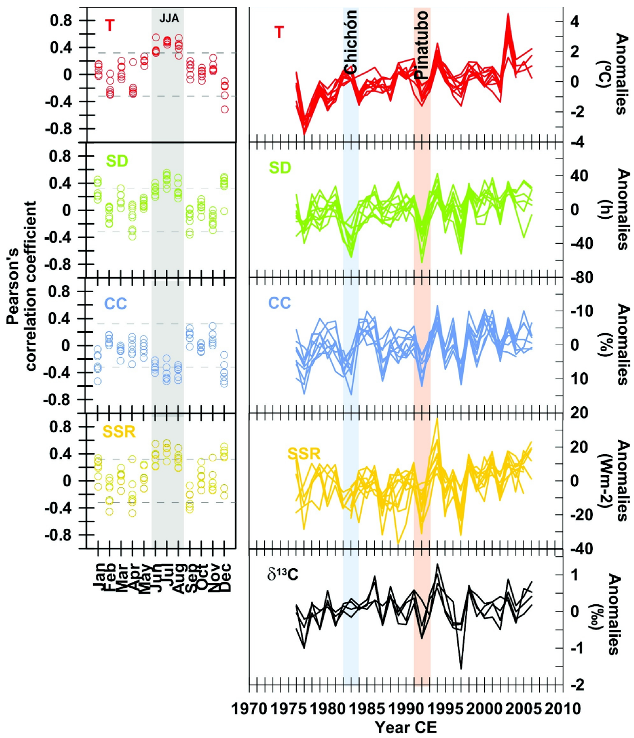

Fig. 3 Left panel: Correlations of $\delta^{13}C$ and a set of stations of mean temperature (T), sunshine duration (SD), downward surface shortwave radiation from station (SSR) and percentage of cloud cover (CC). Summer season is highlighted (JJA). Dashed lines indicate 95% significance levels. Rigtht panel: Interannual variations in the instrumental records of T (red), SD (green), CC (blue), SSR (yellow) and individuals series of $\delta^{13}C$ (black). The El Chichón and Pinatubo volcanic eruptions are highlighted. CC series are inverted for a better visualization.

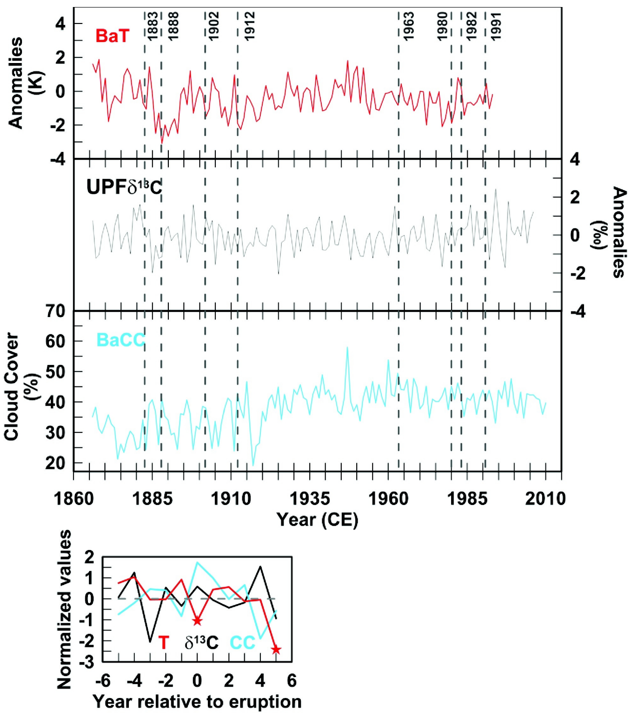

Fig. 4 The top three panels show the volcanic imprint in meteorological series from Barcelona station of temperature (BaT; top panel), percentage of cloud cover (BaCC; bottom panel) and UPF $\delta^{13}C$ (middle panel). Dashed grey lines indicate the 8 large volcanic eruptions considered for the analysis. Bottom left panel shows the result of the SEA analysis performed BaT, BaCC and UPF $\delta^{13}C$. Stars indicate significant departures at 99% level.

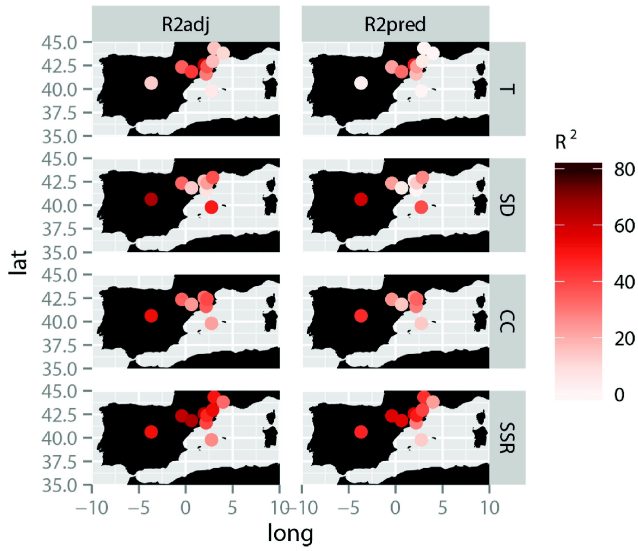

Fig. 5 Spatial patterns of adjusted R^2 (R2adj), predicted R^2 (R2pred) of the regression analysis between each set of instrumental series and UPF $\delta^{13}C$ for the common period 1983-2005. Instrumental series of mean temperature (T), sunshine duration (SD), percentage of cloud cover (CC) and surface solar radiation (SSR). The name of the station, coordinates and the values of R2adj and R2pred are provided in Table 1.

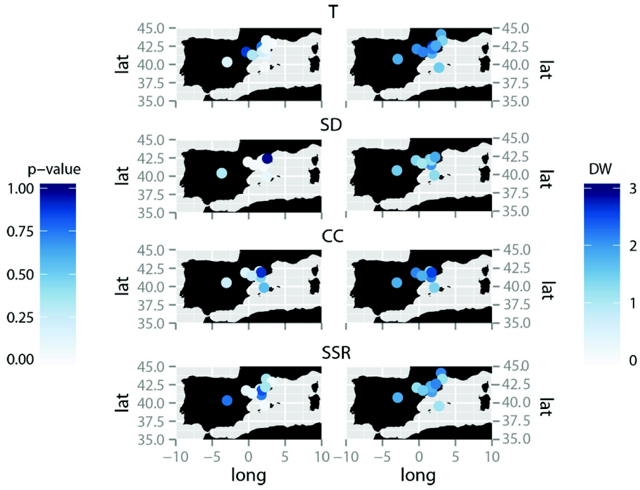

Fig. 6 Spatial patterns of the residual analysis corresponding to the regression between each set of instrumental series and UPF $\delta^{13}C$. The analysis includes the p-value for the trend (left panel) and autocorrelation (DW; right panel) of the residuals resulting from the regression. Abbreviation: mean temperature (T), sunshine duration (SD), percentage of cloud cover (CC) and surface solar radiation (SSR), Durbin-Watson test (DW). Values are provided in Table 1.

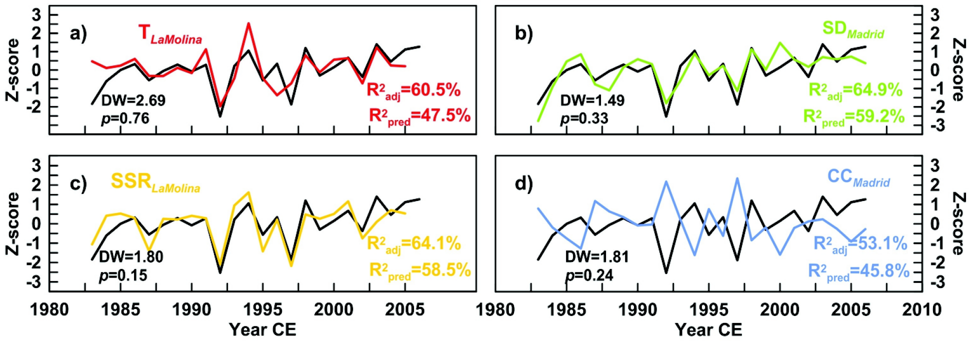

Fig. 7 Linear regression trials between $\delta^{13}C$ (black line) and June-to-August series of a) mean temperature ($T_{LaMolina}$); b) sunshine duration (SD_{Madrid}); c) satellite surface solar radiation from a single grid-cell ($SSR_{LaMolina}$); d) and percentage of cloud cover (CC_{Madrid}) for the common period 1983-2005. Each panel shows the adjusted and predicted R^2, the Durbin-Watson test for residuals autocorrelation (DW) with p-value of the linear trend analysis.

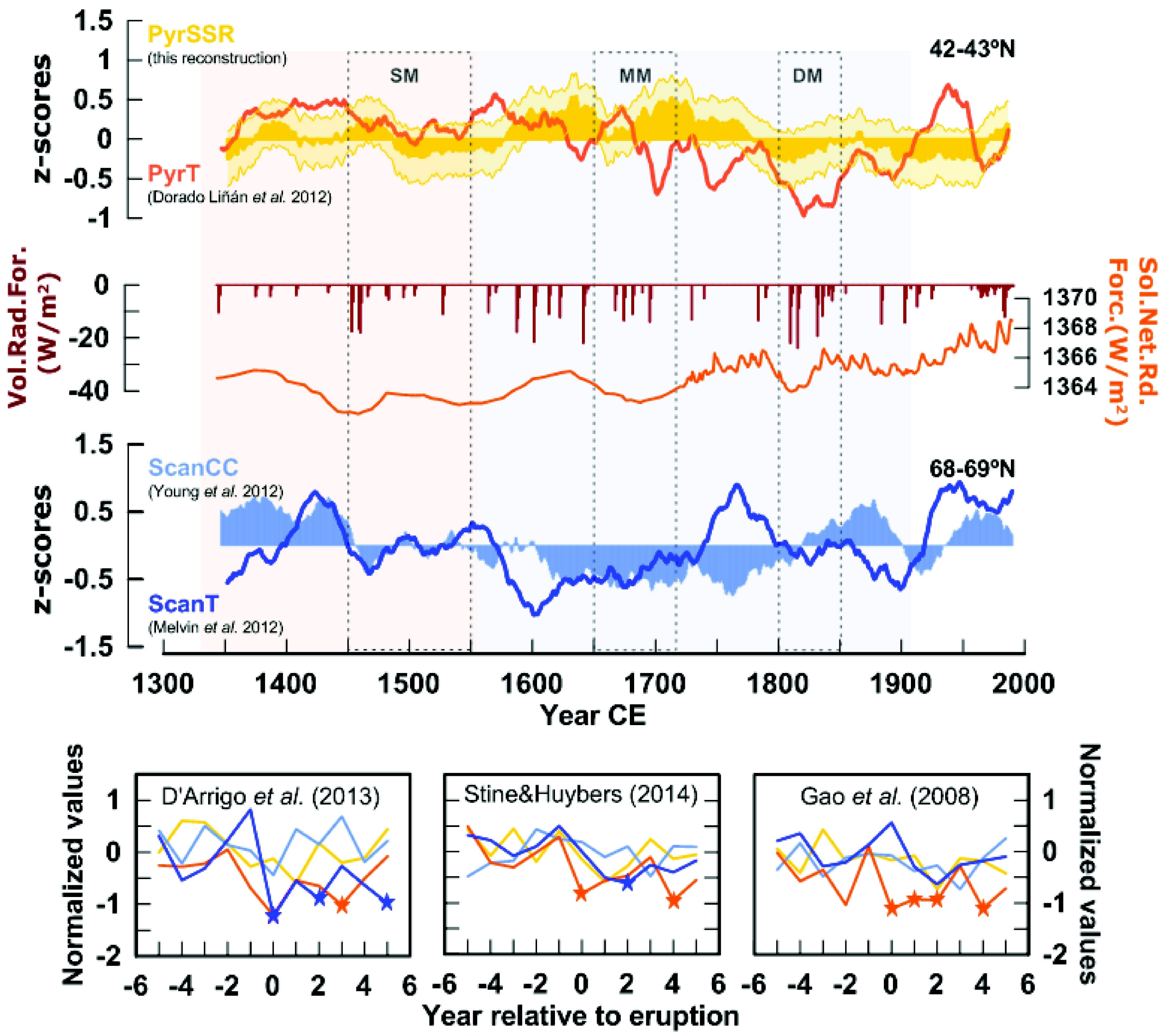

Fig. 8 Top panel show the variations of summer temperatures and sunlight in a latitudinal gradient including variations of summer SSR (PyrSSR) (95% confidence interval) and May to September temperature in the Pyrenees (PyrT); reconstructions of volcanic eruptions from Crowley (2000) and the reconstructions of total solar irradiance (TSI) derived from Crowley (2000) (orange) (middle panel) and tree-ring based temperature (ScanT, in dark blue) and percentage of cloud cover (ScanCC, in light blue) reconstructions in Scandinavia. All series are z-scores smoothed with a 30-year centred moving average. Periods of solar minima are highlighted: WM (Wolf minimum); SM (Spörer Minimum); MM (Maunder Minimum) and DM (Dalton Minimum). Shaded areas indicate Medieval Climate Anomaly (MCA; lightorange) and Little Ice Age (LIA; lightblue). Bottom panel shows the results of the Superposed Epoch Analysis (SEA) using three different sets of volcanos from D'Arrigo et al. (2013) (left), Stine and Huybers (2014) (middle) and Gao et al. (2008) (right). Stars indicate a statistically-significant departure at 95% level.

Variable	Station name/source	Longitude	Latitude	R^2_{adj} (%)	R^2_{pred} (%)	DW	*p*-value residuals trend
T	La Molina	1.96	42.34	**61.7**	**49.9**	2.67	0.76
	Barcelona	2.17	41.39	29.6	17.1	1.76	0.09
	Girona	2.27	42.17	37.6	23.5	2.21	0.22
	Huesca	-0.41	42.13	35.2	22.3	2.07	0.88
	Lleida	0.62	41.62	43.2	32.7	2.17	0.34
	Madrid	-3.68	40.41	13.2	2.9	1.82	0.15
	Mallorca	2.74	39.57	4.5	0.0	1.48	<0.01
	Millau	3.02	44.12	15.8	1.3	1.78	0.06
	Montpellier	3.97	43.58	10.8	0.0	1.40	<0.01
	Perpignan	2.87	42.73	16.7	4.2	1.85	0.05
SD	La Molina	1.96	42.34	16.2	0.0	1.53	0.07
	Barcelona	2.17	41.39	6.9	0.0	2.03	<0.01
	Girona	2.27	42.17	23.2	14.0	1.25	<0.01
	Huesca	-0.41	42.13	33.8	23.3	1.35	<0.01
	Lleida	0.62	41.62	13.8	4.2	1.05	<0.01
	Madrid	-3.68	40.41	**64.9**	**59.2**	1.49	0.33
	Mallorca	2.74	39.57	49.4	38.3	1.28	0.08
	Perpignan	2.87	42.73	37.7	27.0	1.87	0.98
CC	La Molina	1.96	42.34	32.4	26.4	1.33	0.16
	Barcelona	2.17	41.39	35.9	29.6	2.19	0.47
	Girona	2.27	42.17	40.0	34.1	2.57	0.90
	Huesca	-0.41	42.13	34.9	25.3	2.15	0.15
	Lleida	0.62	41.62	24.0	14.9	1.80	0.25
	Madrid	-3.68	40.41	**53.1**	**45.8**	1.81	0.24
	Mallorca	2.74	39.57	22.8	14.2	1.42	0.56
SSR	La Molina(s)	1.96	42.34	**64.1**	**58.5**	1.80	0.15
	Barcelona(s)	2.17	41.39	39.8	29.3	1.95	0.74
	Girona(s)	2.27	42.17	47.0	49.2	1.79	0.83
	Huesca(s)	-0.41	42.13	**62.2**	**56.8**	1.23	0.09
	Lleida(s)	0.62	41.62	**65.3**	**56.2**	1.50	0.06
	Madrid	-3.68	40.41	**52.7**	**47.5**	1.83	0.76
	Mallorca	2.74	39.57	26.7	13.4	1.16	0.03
	Millau	3.02	44.12	**51.3**	**44.6**	2.11	0.35
	Montpellier	3.97	43.58	33.0	23.4	1.20	0.06
	Perpignan	2.87	42.73	**53.7**	**40.3**	2.15	0.35

Table 1. Instrumental series of temperature (T), sunshine duration (SD), percentage of cloud cover (CC) and ground-based surface solar radiation (SSR). The name of the station/source and the coordinates are provided. (s) Refers to SSR data derived from satellite products. The results of the regression analysis between each instrumental series and UPF$\delta^{13}C$ are provided: adjusted R^2 (R^2adj), predicted R^2 (R^2pred) and the residual analysis that includes the Durbin-Watson test (DW) and the p-value for the trend in the residuals from the regression. Bold numbers correspond to R^2adj > 50% and R^2pred> 0.40%.